Phys Chem Minerals (2004) 31: 85–91
DOI 10.1007/s00269-003-0372-9

ORIGINAL PAPER

M. Akaogi · N. Kamii · A. Kishi · H. Kojitani

Calorimetric study on high-pressure transitions in $KAlSi_3O_8$

Received: 25 March 2003 / Accepted: 15 October 2003

Abstract $KAlSi_3O_8$ sanidine dissociates into a mixture of $K_2Si_4O_9$ wadeite, Al_2SiO_5 kyanite and SiO_2 coesite, which further recombine into $KAlSi_3O_8$ hollandite with increasing pressure. Enthalpies of $KAlSi_3O_8$ sanidine and hollandite, $K_2Si_4O_9$ wadeite and Al_2SiO_5 kyanite were measured by high-temperature solution calorimetry. Using the data, enthalpies of transitions at 298 K were obtained as 65.1 ± 7.4 kJ mol^{-1} for sanidine → wadeite + kyanite + coesite and 99.3 ± 3.6 kJ mol^{-1} for wadeite + kyanite + coesite → hollandite. The isobaric heat capacity of $KAlSi_3O_8$ hollandite was measured at 160–700 K by differential scanning calorimetry, and was also calculated using the Kieffer model. Combination of both the results yielded a heat-capacity equation of $KAlSi_3O_8$ hollandite above 298 K as $C_p = 3.896 \times 10^2 - 1.823 \times 10^3 T^{-0.5} - 1.293 \times 10^7 T^{-2} + 1.631 \times 10^9 T^{-3}$ (C_p in J mol^{-1} K^{-1}, T in K). The equilibrium transition boundaries were calculated using these new data on the transition enthalpies and heat capacity. The calculated transition boundaries are in general agreement with the phase relations experimentally determined previously. The calculated boundary for wadeite + kyanite + coesite → hollandite intersects with the coesite–stishovite transition boundary, resulting in a stability field of the assemblage of wadeite + kyanite + stishovite below about 1273 K at about 8 GPa. Some phase–equilibrium experiments in the present study confirmed that sanidine transforms directly to wadeite + kyanite + coesite at 1373 K at about 6.3 GPa, without an intervening stability field of $KAlSiO_4$ kalsilite + coesite which was previously suggested. The transition boundaries in $KAlSi_3O_8$ determined in this study put some constraints on the stability range of $KAlSi_3O_8$ hollandite in the mantle and that of sanidine inclusions in kimberlitic diamonds.

M. Akaogi (✉) · N. Kamii · A. Kishi · H. Kojitani
Department of Chemistry, Gakushuin University,
1-5-1 Mejiro, Toshima-ku, Tokyo, 171–8588, Japan
e-mail: masaki.akaogi@gakushuin.ac.jp
Fax: +81-3-5992-1029
Tel.: +81-3-3986-0221 ext.6462

Keywords High-pressure transition · Thermodynamic property · Kieffer model · Sanidine · Hollandite

Introduction

Potassium feldspar is one of the most abundant minerals in the Earth's crust. Experimental studies have shown that at around 1300 K $KAlSi_3O_8$ feldspar transforms to an assemblage of $K_2Si_4O_9$ wadeite, Al_2SiO_5 kyanite, and SiO_2 coesite at about 6 GPa, and the three phases further recombine into $KAlSi_3O_8$ hollandite at about 9 GPa (Urakawa et al. 1994; Yagi et al. 1994). $K_2Si_4O_9$ wadeite has a structure based on rings of three SiO_4 tetrahedra connected by octahedrally coordinated Si (Kinomura et al. 1977; Swanson and Prewitt 1983). The structure of $KAlSi_3O_8$ hollandite has a large square tunnel formed by double chains of edge-shared $(Si,Al)O_6$ octahedra, and K resides in the tunnel (Ringwood et al. 1967; Yamada et al. 1984).

The hollandite-structured silicate has been considered as a host phase for large cations of geochemical interest such as K, Na, Sr, Ba, and Pb at high pressures and high temperatures (Ringwood 1975; Prewitt and Downs 1998). Recently, hollandite phases with $KAlSi_3O_8$- and $NaAlSi_3O_8$-rich compositions were discovered in shocked meteorites, and the geochemical significance of hollandite in the mantle was discussed (Akaogi 2000; Gillet et al. 2000; Langenhorst and Poirier 2000; Tomioka et al. 2000). Recent studies on high-pressure transitions and melting in potassium-bearing basalts and pelitic rocks indicated the formation of $KAlSi_3O_8$ hollandite at pressures greater than 10 GPa (Schmidt 1996; Domanik and Holloway 1996, 2000; Wang and Takahashi 1999). These experimental results suggest a possible significance for $KAlSi_3O_8$ hollandite in recycling potassium through the subduction of oceanic crust into the deep mantle. Also, the behavior of phases which might host potassium in the deep mantle is of great interest because it is widely accepted that ^{40}K played an important role in heat generation in the Earth's thermal evolution.

Although experimental studies on potassium-bearing silicates have been reported extensively, thermodynamic properties of the potassium-bearing high-pressure phases are still insufficient to elucidate a stable topology of phase relations and to accurately calculate the transition boundaries in the system K_2O–Al_2O_3–SiO_2. In this study, we have measured enthalpies of $KAlSi_3O_8$ sanidine and hollandite and of $K_2Si_4O_9$ wadeite by high-temperature solution calorimetry. The heat capacity of $KAlSi_3O_8$ hollandite was measured, and also estimated from vibrational modeling based on the Kieffer model. Using the resulting thermodynamic data, phase-transition boundaries of $KAlSi_3O_8$ sanidine to the mixture of wadeite, kyanite, and coesite, and further to hollandite are calculated. The possible stability of an assemblage of $KAlSiO_4$ kalsilite and coesite in the $KAlSi_3O_8$ composition is discussed on the basis of phase-equilibrium experiments. The stability of $KAlSi_3O_8$ hollandite and sanidine in the mantle is also discussed.

Experimental

Sample synthesis

The samples for calorimetric measurements were synthesized using reagent grade chemicals as follows. For synthesis of the samples at high pressures and high temperatures, a Kawai-type double-staged multianvil apparatus of Gakushuin University was used, except for $KAlSi_3O_8$ sanidine. Tungsten carbide anvils of 5-, 8-, and 12-mm-edge lengths were used in combination with MgO·5wt%Cr_2O_3 octahedra of 10, 14, and 18 mm in edge, respectively, depending on pressure. A powdered starting material was put into a cylindrical Pt or Re capsule/furnace. The starting material was kept at 5–15 GPa and 1173–1373 K for 1–6 h, quenched isobarically, and recovered to ambient condition. Temperature was measured at the outer surface of the central part of the furnace with a Pt/Pt–13%Rh thermocouple. The effect of pressure on the emf of the thermocouple was not corrected. More detailed description of the high-pressure techniques is given in Akaogi et al. (1999, 2002).

The $KAlSi_3O_8$ sanidine sample synthesized by Urakawa et al. (1994) was kindly provided by Drs. S. Urakawa and T. Taniguchi. The sample was examined by powder X-ray diffraction and analyzed with an electron probe microalalyzer (EPMA), confirming single-phase sanidine.

$K_2Si_4O_9$ wadeite was synthesized from a stoichiometric mixture of K_2CO_3 and SiO_2. The mixture was heated at 973 K for 3 days for decarbonation, melted at 1377 K for 2 h, and quenched to form glass. The glass was crystallized at 5 GPa and 1173 K for 3 h using 12-mm-edge anvils. The synthesized material was confirmed as $K_2Si_4O_9$ wadeite by powder X-ray diffraction and EPMA analysis.

$KAlSi_3O_8$ hollandite was synthesized from a gel starting material prepared by the same method as described by Yagi et al. (1994). K_2CO_3 and Al metal were dissolved in nitric acid, and were mixed with a solution of tetraethyl orthosilicate $(C_2H_5O)_4Si$ in alcohol. Gel precipitated from the solution was dried and heated at about 973 K for 3 h. The heated gel was kept at 15 GPa and 1373 K for 1 h using 5-mm-edge anvils. The recovered sample was examined by powder X-ray diffraction and EPMA analysis, confirming the hollandite phase of $KAlSi_3O_8$ composition, with a very small amount ($< 5\%$) of kyanite as an impurity. The effect of the kyanite on measured thermodynamic properties was ignored because of the small abundance.

A natural kyanite sample from Capelinha, Minas Gerais, Brazil, was used to measure the drop-solution enthalpy. EPMA analysis indicated that the kyanite composition was almost Al_2SiO_5 with a trace amount of FeO (0.19 wt%). The kyanite sample was pulverized and heated in air at 1273 K for 1 h. The heated sample was confirmed to be single-phase kyanite by powder X-ray diffraction, and was used for calorimetric measurements.

Lattice parameters of the above samples of sanidine, wadeite, kyanite, and hollandite were determined by powder X-ray diffraction with Cr Kα radiation (45 kV, 250 mA). High-purity Si was used as the standard to calibrate 2θ. The lattice parameters were refined using 15–32 diffraction lines by the least-squares method.

Two runs of $KAlSi_3O_8$ composition were also made at 5.9 and 6.6 GPa at 1373 K to examine the phase relations, using 8-mm-edge anvils. In the first run, the single phase of $KAlSi_3O_8$ sanidine was kept at 6.6 GPa and 1373 K for 6 h. In the second run, $K_2Si_4O_9$ wadeite and Al_2SiO_5 kyanite described above and SiO_2 coesite synthesized in Akaogi et al. (1995) were thoroughly mixed in the stoichiometric ratios of $KAlSi_3O_8$ composition. This mixture was kept at 5.9 GPa and 1373 K for 5 h. The recovered samples were examined by powder X-ray diffraction and EPMA analysis.

Heat capacity and enthalpy measurements

The heat capacity at constant pressure (C_p) of hollandite was measured at 1 atm using a differential scanning calorimeter (Rigaku, DSC 8230B). The hollandite powder (24.94 mg) and α-Al_2O_3 powder (24.53 mg) were crimped in Al pans. The latter was used as the standard material for heat capacity. The measurement was repeated in two different temperature ranges, 160–390 and 320–700 K, eight and ten times, respectively. In the low-temperature measurements, the sample was first cooled with liquid nitrogen, and then heated at a rate of 6 K min^{-1}. In the high-temperature measurements, the sample was heated from near-room temperature at 7 K min^{-1}. Powder X-ray diffraction confirmed that hollandite retained the structure after the high temperature measurements. The average heat capacities at 10-K interval were obtained, with an average standard deviation of 4.3 J mol^{-1} K^{-1}. More detailed description of the heat–capacity measurements is given in Akaogi et al. (1990).

A twin Calvet-type microcalorimeter (Setaram, HT-1000) operated at 978 ± 1 K was used for the enthalpy measurements at Gakushuin University. Detailed descriptions of the calorimeter and enthalpy measurements are described in Akaogi et al. (1990). A differential drop-solution method described in Akaogi et al. (1995) was adopted, and lead borate ($2PbO·B_2O_3$) solvent was used. In this method, a powder sample of about 5–10 mg was put into a thin silica glass capsule of about 1.5–3 mg with a Pt wire of about 100–140 mg, and dropped from outside the calorimeter at room temperature into the calorimeter detector at 978 K. The sample and capsule then dissolved in the solvent. Simultaneously, another set of silica-glass capsule and Pt wire, without sample, was dropped into the other calorimeter detector, and the capsule was dissolved in the solvent. The weights of the two silica-glass capsules and of the two Pt wires were adjusted to cancel the heat effects in the two detectors of the twin calorimeter. All the samples and silica-glass capsules were completely dissolved in the solvent within about 30 min. The sample amount for each run of differential drop-solution calorimetry was 4.65–5.71 mg for sanidine, 4.75–8.35 mg for wadeite, 7.03–10.65 mg for kyanite, and 4.38–5.98 mg for hollandite.

Results and discussion

Measured enthalpies

The compositions and lattice parameters of sanidine, wadeite, kyanite, and hollandite used for measurements of enthalpy and heat capacity are shown in Table 1.

Table 1 Compositions and lattice parameters of the samples used for calorimetric measurements

Phase	$KAlSi_3O_8$ sanidine	$K_2Si_4O_9$ Wadeite	Al_2SiO_5 kyanite	$KAlSi_3O_8$ hollandite
SiO_2 (wt%)	64.64	71.63	36.22	63.70
Al_2O_3	18.52	–	64.54	19.00
FeO	–	–	0.19	–
K_2O	16.82	27.69	–	16.93
Total	99.98	99.32	100.95	99.63
	O = 8	O = 9	O = 5	O = 8
Si	2.992	4.004	0.970	2.996
Al	1.010	–	2.037	1.043
Fe	–	–	0.004	–
K	0.993	1.975	–	1.006
Total	4.995	5.979	3.011	5.045
a (Å)	8.602(4)	6.614(1)	7.114(5)	9.327(3)
b (Å)	13.024(3)	–	7.847(2)	–
c (Å)	7.186(2)	9.512(1)	5.564(2)	2.724(1)
α (°)	–	–	89.9(6)	–
β (°)	116.05(8)	–	101.1(2)	–
γ (°)	–	–	106.0(1)	–

The cell parameters of sanidine, wadeite, and kyanite are consistent with JCPDS files 25–618, 39–212, and 11–46, respectively. The lattice parameters of hollandite agree with those by Yamada et al. (1984) and Yagi et al. (1994). The drop-solution enthalpies ($\Delta H°_{d\text{-}s}$) measured for the samples are shown in Table 2, together with the data on coesite and stishovite measured by the same techniques by Akaogi et al. (1995). The $\Delta H°_{d\text{-}s}$ of sanidine is consistent with 288.6 ± 0.6 kJ mol^{-1}, which is the sum of the enthalpy of solution of $(K_{0.99}Na_{0.01})AlSi_3O_8$ sanidine measured at 977 K in lead borate by Hovis and Navrotsky (1995) and the heat content ($H°_{978}–H°_{298}$) of sanidine calculated using the heat-capacity equation of Robie and Hemingway (1995). The $\Delta H°_{d\text{-}s}$ of kyanite agrees well with 153.2 ± 0.5 kJ mol^{-1}, the sum of the heat of solution in lead borate at 973 K from Kiseleva et al. (1983) and the heat content of kyanite calculated from the C_p equation of Robie and Hemingway (1995). Differences between the measured drop-solution enthalpies give the enthalpies of transition s at 298 K. Using the $\Delta H°_{d\text{-}s}$ data in Table 2, the transition enthalpies at 298 K ($\Delta H°_{tr,298}$) for the reactions:

Table 2 Measured drop-solution enthalpies. Error is two standard deviations the mean. *Number in brackets* is number of runs

Sample	$\Delta H°_{d\text{-}s}$ (kJ mol^{-1})	Reference
$KAlSi_3O_8$ sanidine	284.13 ± 7.07[6]	a
$K_2Si_4O_9$ wadeite	246.26 ± 2.93[13]	a
Al_2SiO_5 kyanite	155.14 ± 2.89[13]	a
$KAlSi_3O_8$ hollandite	119.75 ± 2.94[5]	a
SiO_2 coesite	36.65 ± 0.43[10]	b
SiO_2 stishovite	3.04 ± 0.91[6]	b

a This study; b Akaogi et al. (1995)

$$KAlSi_3O_8(san) \rightarrow 1/2K_2Si_4O_9(wa) + 1/2Al_2SiO_5(ky) + 1/2SiO_2(co) \quad (1)$$

$$1/2K_2Si_4O_9(wa) + 1/2Al_2SiO_5(ky) + 1/2SiO_2(co) \rightarrow KAlSi_3O_8(hol) \quad (2)$$

are obtained to be 65.1 ± 7.4 and 99.3 ± 3.6 kJ mol^{-1}, respectively. $\Delta H°_{tr,298}$ for Eq. (1) is consistent with the calorimetric datum by Geisinger et al. (1987), 72.6 ± 5.5 kJ mol^{-1}, within the errors. We calculated the enthalpy of formation at 298 K ($\Delta H°_{f,298}$) of $KAlSi_3O_8$ hollandite from elements by combining our data for Eq. (1) and (2) with the $\Delta H°_{f,298}$ of sanidine by Robie and Hemingway (1995), resulting in −3801 ± 8 kJ mol^{-1}. This value is considerably higher than −3921.2 kJ mol^{-1} estimated by Domanik and Holloway (2000) using the phase-relation data.

Measured heat capacity and vibrational modeling

The measured molar heat capacity (C_p) of $KAlSi_3O_8$ hollandite as a function of temperature is shown in Table 3 and Fig. 1. C_p increases from 98.3 J mol^{-1} K^{-1} at 160 K to 305.9 J mol^{-1} K^{-1} at 700 K. Next, we have calculated the heat capacity of hollandite using the lattice vibrational model by Kieffer (1979b, 1980). $KAlSi_3O_8$ hollandite has $I4/m$ symmetry (Ringwood et al. 1967; Yamada et al. 1984), and its primitive unit cell contains 13 atoms. In 39 degrees of freedom in total, three are acoustic modes, and the rest are optic modes. Because acoustic velocities of $KAlSi_3O_8$ hollandite have not yet been measured, we first estimated a compressional velocity (V_p) of 10.04 km s^{-1}, using Birch' s (1961) law on the compressional velocity vs. density (ρ) [V_p(km s^{-1}) = −1.87 + 3.05 ρ (g cm^{-3})]. Shear velocity (V_s) was evaluated as 6.41 km s^{-1}, using the above V_p

Table 3 Measured heat capacities of $KAlSi_3O_8$ hollandite

T (K)	C_p (J mol^{-1}K^{-1})	*T* (K)	C_p (J mol^{-1}K^{-1})	*T* (K)	C_p (J mol^{-1}K^{-1})
160	98.33	350	226.13	540	280.50
170	105.98	360	231.56	550	282.02
180	112.01	370	235.15	560	283.79
190	122.37	380	238.70	570	286.18
200	126.86	390	242.52	580	287.88
210	139.82	400	245.24	590	289.33
220	148.22	410	246.72	600	291.32
230	154.12	420	251.97	610	290.44
240	161.99	430	254.59	620	292.64
250	166.13	440	258.20	630	294.27
260	176.60	450	260.94	640	297.50
270	182.77	460	262.83	650	298.55
280	187.24	470	265.79	660	299.48
290	193.62	480	268.44	670	301.29
300	200.49	490	270.19	680	304.06
310	204.86	500	272.59	690	303.43
320	211.96	510	272.98	700	305.87
330	214.98	520	277.57		
340	220.42	530	278.26		

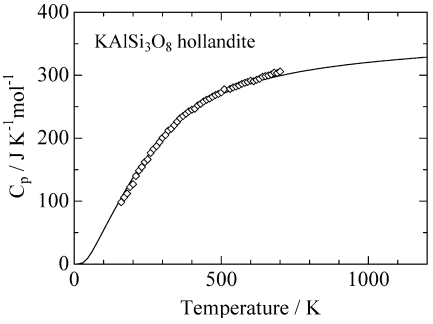

Fig. 1 Molar heat capacities (C_p) of $KAlSi_3O_8$ hollandite at 1 atm. *Open diamonds* show the measured heat capacities, and a *solid curve* the calculated C_p using the Kieffer model

value and measured bulk modulus (K_0) of 180 GPa (Zhang et al. 1993). Directionally averaged acoustic velocities (u_1, u_2, u_3) were obtained as 6.05, 6.87 and 10.04 km s^{-1}, respectively, from the V_p and V_s values using the method by Kieffer (1979a), where we have made use of the well-known structural similarity between hollandite and rutile.

Infrared and Raman spectra are generally used for modeling of optic modes. However, only the Raman spectrum has been reported for $KAlSi_3O_8$ hollandite (Gillet et al. 2000), and we used this to constrain the optic modes. The reported Raman spectra showed several bands in the wavenumber range from about 200 to 975 cm^{-1}. Because the lower limit of the spectrum range was not well constrained, we adopted it as an adjustable parameter ω_1. We constructed a single optic continuum model in the range from the lower cutoff wavenumber (ω_1) to 975 cm^{-1}. The heat capacity at constant volume (C_v) was calculated on the basis of the model of acoustic and optic modes described above. To calculate C_p from C_v, we used the equation $C_p = C_v + TV\alpha^2K_0$, where T, V, and α are temperature, molar volume, and thermal expansion coefficient, respectively. Thermal expansion coefficients are given in Table 4. ω_1 of the optic continuum was determined as 160 cm^{-1} as this gave the best fit between the observed C_p (Table 3) and calculated C_p values. Calculated values of C_p agree well with the measured C_p within the standard deviation of the measured C_p. We further fitted a heat-capacity equation by Berman and Brown (1985) to the calculated C_p over the range 298–1500 K, as (C_p in J $mol^{-1}K^{-1}$, T in K):

$$C_p = 3.896 \times 10^2 - 1.823 \times 10^3 T^{-0.5} - 1.293 \times 10^7 T^{-2} + 1.631 \times 10^9 T^{-3} \quad (3)$$

Equilibrium phase relations in $KAlSi_3O_8$

High-pressure phase transitions in $KAlSi_3O_8$ were examined in detail at 5–12 GPa by Yagi et al. (1994) and Urakawa et al. (1994). The latter determined the pressures by in situ X-ray measurements on the basis

Table 4 Physical properties of the phases in the system K_2O–Al_2O_3–SiO_2 used for phase-boundary calculation

Phase	V°_{298}	$\alpha = a_0 + a_1T + a_2T^{-2}$ (K^{-1})			K_{0T}	K'_{0T}
	(cm^3 mol^{-1})	$a_0 \times 10^5$	$a_1 \times 10^9$	a_2	(GPa)	
$KAlSi_3O_8$ (san)	109.05[a]	1.297	8.683	0[d]	67[j]	4[k]
$K_2Si_4O_9$ (wa)	108.44[b]	2.950	0	0[e]	90[l]	4[k]
Al_2SiO_5 (ky)	44.15[a]	2.505	0	0[f]	190[m]	4[k]
SiO_2 (co)	20.64[a]	0.543	5.000	0[g]	97[n]	4.3[n]
SiO_2 (st)	14.01[a]	1.574	7.886	0.150[h]	302[o]	5.3[o]
$KAlSi_3O_8$ (hol)	71.28[c]	3.300	0	0[i]	180[p]	4[k]

Phase	$C_p = c_1 + c_2T^{-0.5} + c_3T^{-2} + c_4T^{-3}$ (J $mol^{-1}K^{-1}$)			
	$c_1 \times 10^{-2}$	$c_2 \times 10^{-3}$	$c_3 \times 10^{-6}$	$c_4 \times 10^{-8}$
$KAlSi_3O_8$ (san)	4.023	−2.639	−7.723	11.088[a]
$K_2Si_4O_9$ (wa)	4.991	−4.350	0	0[q]
Al_2SiO_5 (ky)	2.449	−1.295	−7.109	8.407[a]
SiO_2 (co)	0.789	−0.164	−5.065	8.250[r]
SiO_2 (st)	0.858	−0.346	−3.605	4.511[r]
$KAlSi_3O_8$ (hol)	3.896	−1.823	−12.934	16.307[s]

[a] Robie and Hemingway (1995)
[b] Swanson and Prewitt (1983)
[c] Yamada et al. (1984)
[d] Skinner (1966)
[e] Swanson and Prewitt (1986)
[f] Winter and Ghose (1979)
[g] Saxena et al. (1993)
[h] Ito et al. (1974)
[i] α at 1 atm calculated from Urakawa et al.'s (1994) data
[j] Angel et al. (1988)
[k] Assumed
[l] Geisinger et al. (1987)
[m] Yang et al. (1997)
[n] Angel et al. (2001)
[o] Li et al. (1996)
[p] Zhang et al. (1993)
[q] Fasshauer et al. (1998)
[r] Akaogi et al. (1995)
[s] This study

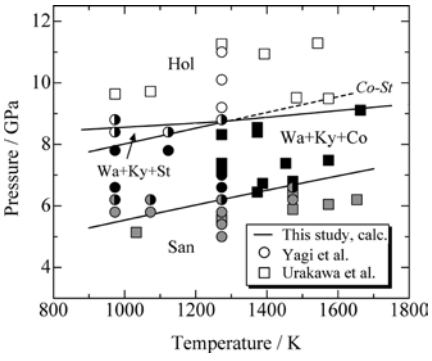

Fig. 2 Phase relations in $KAlSi_3O_8$. *Solid lines* represent calculated transition boundaries using thermodynamic data in this study, and a *dashed line* shows the coesite–stishovite transition boundary from Zhang et al. (1996). *Circles* represent experimental runs by Yagi et al. (1994) after pressure correction, and *squares* by Urakawa et al. (1994). *Shaded, closed, and open symbols* show sanidine, wadeite + kyanite + coesite(or stishovite), and hollandite, respectively. *San* Sanidine; *Wa* wadeite; *Ky* kyanite; *Co* coesite; *St* stishovite; *Hol* hollandite

of an NaCl pressure scale. However, in the quench experiments by Yagi et al. (1994), transition pressures were determined in the range 7–10 GPa at high temperatures, based mostly on determination using the coesite–stishovite transition by Yagi and Akimoto (1976). Zhang et al. (1996) redetermined the equilibrium boundary of the coesite–stishovite transition more accurately on the NaCl scale, and the transition boundary is consistent with calorimetric studies (Akaogi et al. 1995; Liu et al. 1996). The coesite–stishovite transition pressure at 1273 K was 9.1 GPa as given by Yagi and Akimoto (1976), but 8.7 GPa as given by Zhang et al. (1996). We therefore revised the pressure values of phase equilibrium experiments of $KAlSi_3O_8$ by Yagi et al. (1994), using the coesite–stishovite transition pressure by Zhang et al. (1996). The revised results of Yagi et al. (1994) are shown in Fig. 2 together with the data of Urakawa et al. (1994).

Next, we calculated the equilibrium boundaries of transitions (1) and (2), using the transition enthalpies and heat capacity obtained above and the revised phase relations shown in Fig. 2. The transition boundary is defined by the equation:

$$\Delta G(P,T) = \Delta H_T^\circ - T\Delta S_T^\circ + \int_{1\ \mathrm{atm}}^{P} \Delta V(P',T)dP' = 0, \quad (4)$$

where $\Delta G(P, T)$ and $\Delta V(P, T)$ are free energy and molar volume differences, respectively, at P and T. ΔH_T° and ΔS_T° are the enthalpy and entropy of transition, respectively, at 1 atm and temperature T. Using ΔH_T° and one (P, T) point on the assumed equilibrium boundary, we calculated ΔS_T° and the slope of the boundary. Effects of temperature on ΔH_T° and ΔS_T° were corrected using heat capacities of the relevant phases, and the effect of pressure on molar volume was corrected using the third-order Birch-Murnaghan equation of state with bulk moduli and their pressure derivatives. The effect of temperature was calculated using thermal expansion coefficients. The heat capacities, thermal expansivities, and bulk moduli and the pressure derivatives of the relevant phases in the system K_2O–Al_2O_3–SiO_2 are listed in Table 4. More details on the calculation method of phase boundary are given in Akaogi et al. (1995). We adopted 6.2 GPa and 1273 K on the boundary of sanidine → wadeite + kyanite + coesite, and 8.7 GPa and 1273 K on the boundary of wadeite + kyanite + coesite → hollandite. The calculated ΔS°_{298} for the transitions (1) and (2) are –49.0 ± 5.8 and –18.5 ± 2.8 J $mol^{-1}K^{-1}$, respectively. The calculated boundaries are shown in Fig. 2, and the boundary slopes are 2.4 ± 0.3 and 1.1 ± 0.2 MPa K^{-1} for Eqs. (1) and (2), respectively, where the uncertainties of the slopes result from the errors of the measured enthalpies.

The calculated boundary for the sanidine → wadeite + kyanite + coesite transition in Fig. 2 has a slightly steeper gradient than that defined by the experiments by Yagi et al. (1994) and Urakawa et al. (1994). The difference may result from uncertainties in the thermal expansivities, bulk moduli, and heat capacities of wadeite and kyanite that have not been very accurately determined. The sluggish reaction at temperature below about 1100 K in the phase-transition experiments might also be one of the reasons for the difference. The calculated boundary of the wadeite + kyanite + coesite → hollandite transition is almost consistent with the experimental data. At about 8.7 GPa and 1273 K, the boundary for wadeite + kyanite + coesite → hollandite intersects with the coesite–stishovite transition boundary from Zhang et al. (1996). This indicates that an assemblage of wadeite, kyanite, and stishovite is stable in a narrow field below about 1273 K. $\Delta H^\circ_{tr,298}$ for the transition:

$$1/2K_2Si_4O_9(\mathrm{wa}) + 1/2Al_2SiO_5(\mathrm{ky}) + 1/2SiO_2(\mathrm{st}) \rightarrow KAlSi_3O_8(\mathrm{hol}) \quad (5)$$

was calculated to be 82.5 ± 3.6 kJ mol^{-1}, using the data in Table 2. Using this value and the crossing point, ΔS°_{298} of Eq. (5) was calculated as –11.0 ± 2.8 J mol^{-1} K^{-1} and the slope of (5) as 0.8 ± 0.3 MPa K^{-1}. The calculated boundary for transition (5) is shown in Fig. 2. Because the slopes of the reactions (2) and (5) are very similar, the hollandite formation reaction in Fig. 2 looks like an almost straight line. It is interesting that Yagi et al. (1994) and Urakawa et al. (1994) had already found the occurrence of stishovite with wadeite and kyanite in some runs at 8–9 GPa and 950–1300 K. This observation would be consistent with the presence of the field of wadeite + kyanite + stishovite in Fig. 2.

Fasshauer et al. (1998) developed an internally consistent thermodynamic dataset for the system K_2O–Al_2O_3–SiO_2, using available calorimetric and phase-equilibrium data. On the basis of their dataset, they

suggested that $KAlSi_3O_8$ feldspar would dissociate first to $KAlSiO_4$ kalsilite + coesite at 5–6 GPa at temperatures above 823 K and then change to the mixture of wadeite, kyanite, and coesite at higher pressure. Their calculated result is inconsistent with the experimental work of Yagi et al. (1994) and Urakawa et al. (1994), who reported that sanidine directly dissociates to a mixture of wadeite, kyanite, and coesite at 973–1673 K, at 5–7 GPa. The transition boundaries proposed by Fasshauer et al. (1998) are shown in Fig. 3 for comparison with our calculated boundaries. To test the suggestion by Fasshauer et al. (1998), we made two experimental runs at 1373 K at 5.9 and 6.6 GPa. Both of the runs are in the field of kalsilite + coesite proposed by Fasshauer et al. (1998), as shown in Fig. 3, but they are below and above our boundary for the transition of sanidine to wadeite + kyanite + coesite. In the first run at 6.6 GPa and 1373 K for 6 h, single-phase sanidine of $KAlSi_3O_8$ transformed in part to the mixture of wadeite, kyanite, and coesite, but no kalsilite was detected in the run product. In the second run at 5.9 GPa and 1373 K for 5 h using the mixture of wadeite, kyanite, and coesite as the starting material, almost single-phase sanidine, with very small amounts of wadeite, kyanite, and coesite was observed in the run product, but no kalsilite was found. The results of the normal and reverse runs indicate that the phase boundary of sanidine to wadeite + kyanite + coesite represents the equilibrium transition boundary, and this strongly suggests that the assemblage kalsilite + coesite is not stable at temperatures at and below 1373 K. It is suggested that the narrow field of kalsilite + coesite would be sensitive to the small variation in thermodynamic data used in the calculation, because the triple point of Fasshauer et al.'s boundaries could move about 500–600 degrees in temperature due to changes of enthalpy and entropy data with the estimated uncertainties.

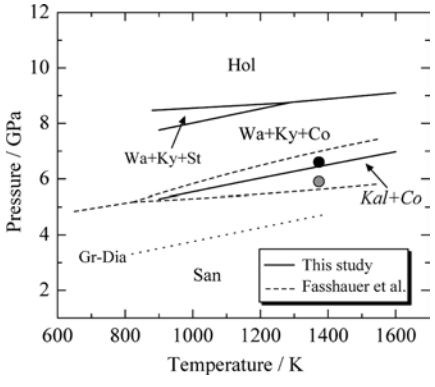

Fig. 3 Phase boundaries in $KAlSi_3O_8$. *Solid lines* are transition boundaries determined in this study. *Dashed lines* represent phase boundaries proposed by Fasshauer et al. (1998) in which a narrow field of kalsilite(Kal) + coesite(Co) appears above about 823 K between the field of sanidine and that of wadeite + kyanite + coesite. *Two circles* show experimental runs in this study. The *closed and shaded circles* represent normal and reverse runs, respectively, for the reaction of sanidine ↔ wadeite + kyanite + coesite, see text. A *thin dotted line* (Gr-Dia) shows the graphite–diamond transition boundary by Kennedy and Kennedy (1976)

$KAlSi_3O_8$ phases in the mantle and meteorites

Our study indicates that $KAlSi_3O_8$ hollandite is stable at pressures above 8.5–9 GPa at 1000–1600 K. This is consistent with the stability of K-rich hollandite at pressures above about 9–10 GPa at 1100–1300 K in sediments reported by Domanik and Holloway (1996, 2000) and in hydrous mid-ocean ridge basalt by Schmidt (1996) and by Wang and Takahashi (1999). Tutti et al. (2000) demonstrated that $KAlSi_3O_8$ hollandite was synthesized at pressure–temperature conditions up to 95 GPa and 2600 K. All these results suggest that hollandite can be stable in the depth range from about 250 km to at least 2200 km in the mantle as a possible K-host phase, when basalts and sediments are entrained into the deep mantle by slab subduction.

Langenhorst and Poirier (2000) discovered $KAlSi_3O_8$ hollandite coexisting with stishovite in melt veins of the shocked meteorite Zagami. They also reported the absence of coesite in the meteorite. These observations are consistent with the stability field of hollandite in the phase diagram shown in Fig. 2, where the formation boundary of $KAlSi_3O_8$ hollandite is very close to the coesite–stishovite transition boundary.

Sanidine crystals with compositions close to $KAlSi_3O_8$ have been found as inclusions in natural diamonds in some kimberlites such as the Sloan kimberlite, Colorado, and the Shengli kimberlite, China (Meyer and McCallum 1986; Wang 1998). Comparing the stability limit of sanidine and the graphite–diamond transition boundary (Kennedy and Kennedy, 1976) in Fig. 3, we suggest that the sanidine crystals were incorporated into the diamonds at pressure of about 4–7 GPa in the mantle, when the continental mantle geotherm is used.

Acknowledgements We are grateful to S. Urakawa and T. Taniguchi for providing the synthetic sanidine sample. We also thank A. Kubo and T. Suzuki for their help in EPMA analysis, and N. Ishizaka and A. Tanaka for their help in calorimetric measurements of some samples. Constructive comments by M. Carpenter and J. Majzlan were helpful in improving the manuscript. We thank J. Tyburczy for editorial handling. This work was supported in part by the Grants-in-Aid from the Ministry of Education, Science, and Culture of Japan and from the Japan Society for the Promotion of Science.

References

Akaogi M (2000) Clues from a shocked meteorite. Science 287: 1602–1603

Akaogi M, Yusa H, Ito E, Yagi T, Suito K, Iiyama JT (1990) The $ZnSiO_3$ clinopyroxene-ilmenite transition: heat capacity, enthalpy of transition and phase equilibria. Phys Chem Miner 17: 17–23

Akaogi M, Yusa H, Shiraishi K, Suzuki T (1995) Thermodynamic properties of α-quartz, coesite, and stishovite and equilibrium phase relations at high pressures and high temperatures. J Geophys Res 100: 22337–22347

Akaogi M, Hamada Y, Suzuki T, Kobayashi M, Okada M (1999) High-pressure transitions in the system $MgAl_2O_4$–$CaAl_2O_4$: a new hexagonal aluminous phase with implication for the lower mantle. Phys Earth Planet Inter 115: 67–77

Akaogi M, Tanaka A, Kobayashi M, Fukushima N, Suzuki T (2002) High-pressure transformations in $NaAlSiO_4$ and thermodynamic properties of jadeite, nepheline, and calcium ferrite-type phase. Phys Earth Planet Inter 130: 49–58

Angel RJ, Hazen RM, McCormick TC, Prewitt CT, Smyth JR (1988) Comparative compressibility of end-member feldspars. Phys Chem Miner 15: 313–318

Angel RJ, Mosenfelder JL, Shaw CSJ (2001) Anomalous compression and equation of state of coesite. Phys Earth Planet Inter 124: 71–79

Berman RG, Brown TH (1985) Heat capacity of minerals in the system Na_2O–K_2O–CaO–MgO–FeO–Fe_2O_3–Al_2O_3–SiO_2–TiO_2–H_2O–CO_2: representation, estimation, and high-temperature extrapolation. Contr Min Petrol 89: 168–183

Birch F (1961) The velocity of compressional waves in rocks to 10 kilobars, part 2. J Geophys Res 66: 2199–2224

Domanik KJ, Holloway JR (1996) The stability and composition of phengitic muscovite and associated phases from 5.5 to 11 GPa: implications for deeply subducted sediments. Geochim Cosmochim Acta 60: 4133–4150

Domanik KJ, Holloway JR (2000) Experimental synthesis and phase relations of phengitic muscovite from 6.5 to 11 GPa in a calcareous metapelite from the Dabie Mountains, China. Lithos 52: 51–77

Fasshauer DW, Wunder B, Chatterjee ND, Hohne GWH (1998) Heat capacity of wadeite-type $K_2Si_4O_9$ and the pressure-induced stable decomposition of K-feldspar. Contrib Min Petrol 131: 210–218

Geisinger KL, Ross NL, McMillan P, Navrotsky A (1987) $K_2Si_4O_9$: energetics and vibrational spectra of glass, sheet silicate and wadeite-type phases. Am Mineral 72: 984–994

Gillet P, Chen M, Dubrovinsky L, El Goresy A (2000) Natural $NaAlSi_3O_8$–hollandite in the shocked Sixiangkou meteorite. Science 287: 1633–1636

Hovis GL, Navrotsky A (1995) Enthalpies of mixing for disordered alkali feldspars at high temperature: a test of regular solution thermodynamic models and a comparison of hydrofluoric acid and lead borate solution calorimetric techniques. Am Mineral 80: 280–284

Ito H, Kawada K, Akimoto S (1974) Thermal expansion of stishovite. Phys Earth Planet Inter 8: 277–281. Erratum 9: 371

Kennedy CS, Kennedy GC (1976) The equilibrium boundary between graphite and diamond. J Geophys Res 81: 2467–2470

Kieffer SW (1979a) Thermodynamics and lattice vibrations of minerals, 1. Mineral heat capacities and their relationships to simple lattice vibrational models. Rev Geophys Space Phys 17: 1–19

Kieffer SW (1979b) Thermodynamics and lattice vibrations of minerals, 3. Lattice dynamics and an approximation for minerals with application to simple substances and framework silicates. Rev Geophys Space Phys 17: 35–59

Kieffer SW (1980) Thermodynamics and lattice vibrations of minerals, 4. Application to chain and sheet silicates and orthosilicates. Rev Geophys Space Phys 18: 862–886

Kinomura N, Koizumi, M, Kume, S (1977) Crystal structures of phases produced by disproportionation of K-feldspar under pressure. In: Manghnani MH, Akimoto S (eds) High-pressure research: application in geophysics. Academic Press, New York, pp 183–189

Kiseleva IA, Ostapenko GT, Ogorodova LP, Topor ND, Timoshkova LP (1983) High-temperature calorimetric data on the andalusite-kyanite-sillimanite-mulite phase equilibria. Geokhimiya 9: 1247–1256

Langenhorst F, Poirier JP (2000) ''Eclogitic'' minerals in a shocked basaltic meteorite. Earth Plane t Sci Lett 176: 259–265

Li B, Rigden SM, Liebermann RC (1996) Elasticity of stishovite at high pressure. Phys Earth Planet Inter 96: 113–127

Liu J, Topor L, Zhang J, Navrotsky A, Liebermann RC (1996) Calorimetric study of the coesite-stishovite transformation and calculation of the phase boundary. Phys Chem Miner 23: 11–16

Meyer HOA, McCallum ME (1986) Inclusions in diamonds from the Sloan kimberlite, Colorado, USA. J Geol 94: 600–612

Prewitt CT, Downs RT (1998) High-pressure crystal chemistry. Rev Mineral 37: 283–312

Ringwood AE (1975) Composition and petrology of the Earth's mantle. McGraw-Hill, New York, 618 pp

Ringwood AE, Reid AF, Wadsley AD (1967) High-pressure $KAlSi_3O_8$, an alumino-silicate with sixfold coordination. Acta Crystallogr 23: 1093–1095

Robie RA, Hemingway BS (1995) Thermodynamic properties of minerals and related substances at 298.15 K and 1 bar (10^5 pascals) pressure and at higher temperatures. US Geol Surv 2131, 461 pp

Saxena SK, Chatterjee N, Fei Y, Shen G (1993) Thermodynamic data on oxides and silicates. Springer, Berlin Heidelberg, New York, 428 pp

Schmidt M (1996) Experimental constraints on recycling of potassium from subducted oceanic crust. Science 272: 1927–1930

Skinner BJ (1966) Thermal expansion. In: Clark SP (ed) Handbook of physical constants. Geol Soc Am Mem 97: 75–96

Swanson DK, Prewitt CT (1983) The crystal structure of $K_2Si^{VI}Si_3^{IV}O_9$. Am Mineral 68: 581–585

Swanson DK, Prewitt CT (1986) Anharmonic thermal motion in $K_2Si^{VI}Si_3^{IV}O_9$. EOS Trans American Geophysical Union, vol 67 Washington pp 369

Tomioka N, Mori H, Fujino K (2000) Shock-induced transition of $NaAlSi_3O_8$ feldspar into a hollandite structure in a L6 chondrite. Geophys Res Lett 27: 3997–4000

Tutti F, Dubrovinsky LS, Saxena SK, Carlson S (2001) Stability of $KAlSi_3O_8$ hollandite-type structure in the Earth's lower mantle conditions. Geophys Res Lett 28: 2735–2738

Urakawa S, Kondo T, Igawa N, Shimomura O, Ohno H (1994) Synchrotron radiation study on the high-pressure and high-temperature phase relations of $KAlSi_3O_8$. Phys Chem Miner 21: 387–391

Wang W (1998) Formation of diamond with mineral inclusions of ''mixed'' eclogite and peridotite paragenesis. Earth Planet Sci Lett 160: 831–843

Wang W, Takahashi E (1999) Subsolidus and melting experiments of a K-rich basaltic composition to 27 GPa: implication for the behavior of potassium in the mantle. Am Mineral 84: 357–361

Winter JK, Ghose S (1979) Thermal expansion and high-temperature crystal chemistry of the Al_2SiO_5 polymorphs. Am Mineral 64: 573–586

Yagi T, Akimoto S (1976) Direct determination of coesite—stishovite transition by in situ X-ray measurements. Tectonophys 35: 259–270

Yagi A, Suzuki T, Akaogi M (1994) High-pressure transitions in the system $KAlSi_3O_8$– $NaAlSi_3O_8$. Phys Chem Minerals 21: 12–17

Yamada H, Matsui Y, Ito E (1984) Crystal-chemical characterization of $KAlSi_3O_8$ with the hollandite structure. Mineral J 12: 29–34

Yang H, Downs RT, Finger LW, Hazen RM, Prewitt CT (1997) Compressibility and crystal structure of kyanite, Al_2SiO_5, at high pressure. Am Mineral 82: 467–474

Zhang J, Ko J, Hazen RM, Prewitt CT (1993) High-pressure crystal chemistry of $KAlSi_3O_8$ hollandite. Am Mineral 78: 493–499

Zhang J, Li B, Utsumi W, Liebermann RC (1996) In situ X-ray observations of the coesite–stishovite transition: reversed phase boundary and kinetics. Phys Chem Miner 23: 1–10